Test of the notch technique for determining the radial sensitivity of the optical model potential *

Lei Yang(杨磊) Cheng-Jian Lin(林承键)[1)] Hui-Ming Jia(贾会明) Xin-Xing Xu(徐新星)
Nan-Ru Ma(马南茹) Li-Jie Sun(孙立杰) Feng Yang(杨峰) Huan-Qiao Zhang(张焕乔)
Zu-Hua Liu(刘祖华) Dong-Xi Wang(王东玺)
China Institute of Atomic Energy, Department of Nuclear Physics, Beijing 102413, China

Abstract: Detailed investigations on the notch technique are performed on ideal data generated by the optical model potential parameters extracted from the ^{16}O+^{208}Pb system at the laboratory energy of 129.5 MeV, to study the sensitivities of this technique to the model parameters as well as the experimental data. It is found that for the perturbation parameters, a sufficiently large reduced fraction and an appropriate small perturbation width are necessary to determine the accurate radial sensitivity; while for the potential parameters, almost no dependence was observed. For the experimental measurements, the number of data points has little influence for heavy target systems, and the relative inner information of the nuclear potential can be derived when the measurement is extended to a lower cross section.

Keywords: optical model potential, notch technique, sensitive region, elastic scattering

PACS: 24.10.Ht, 25.70.Bc **DOI:** 10.1088/1674-1137/40/5/056201

1 Introduction

The optical model potential (OMP) is the most fundamental ingredient in the study of nuclear reaction mechanisms [1]. Nowadays, with the development of radioactive ion beams (RIBs), studies of the OMPs for weakly-bound systems have attracted particular interest, and several abnormal properties have been observed, such as the break-up threshold anomaly (BTA) [2, 3].

The OMP parameters can be extracted effectively by fitting elastic scattering data. However, for a given elastic scattering angular distribution, there exist numerous different families of OMP parameters that can all give successful descriptions of the experimental data, which is the so-called Igo ambiguity [4]. It is meaningful to discuss the OMP only within the sensitive region [5], where the OMP parameters can be determined accurately by the elastic scattering. Therefore, it is important to know what radial regions of the nuclear potential can be well mapped by the analysis of elastic scattering data before making any discussion of the potential.

There are several ways to extract the radial region of the potential sensitivity [5–7]. The frequently used method is to find the crossing-point radius of the potential [7, 8]. However, such a sharply-defined sensitive radius is incompatible with the principles of quantum mechanics, and its value varies with different radial form factors adopted for the OMP [9]. Conflicting results are often brought out, e.g. multi-crossing points [8, 10], especially for energies close to the Coulomb barrier.

In Ref. [5], a notable technique, the notch-perturbation method, was developed, which permits an intuitive investigation of the sensitive region of the OMP. Although the notch technique possesses evident advantages, only a few works [8, 11, 12] have adopted this method to analyze the radial sensitivity of the OMP. In Refs. [5, 11], the importance of the selection of the perturbation parameters has been suggested. However, the dependence of this technique on parameters related to the perturbation, the OMP, and the experimental measurement has not been investigated so far. In the present work, a detailed inspection of the notch technique is performed, in order to lay a more reliable foundation for extending the application of this technique.

2 The notch technique

The principle of the notch technique is to introduce a localized perturbation into either the real or imaginary radial potential, and move the notch radially through the

Received 12 August 2015
∗ Supported by National Natural Science Foundation of China (11375268, 11475263, U1432246 and U1432127) and the National Key Basic Research Program of China (2013CB834404)
1) E-mail: cjlin@ciae.ac.cn

potential to investigate the influence arising from this perturbation on the predicted cross section [5].

The nuclear potential is defined as

$$U_{\rm N} = V(r) + {\rm i}W(r) = -V_0 f_{\rm V}(r) - iW_0 f_{\rm W}(r), \quad (1)$$

where the V_0 and W_0 are depths of the real and imaginary parts of the potential with Woods-Saxon form $f_i(r,a,R)$,

$$f_i(r,a,R) = \left[1+\exp\left(\frac{r-R_i}{a_i}\right)\right]^{-1}, i = V,W, \quad (2)$$

where $R_i = r_{0i}(A_{\rm P}^{1/3}+A_{\rm T}^{1/3})$, and $A_{\rm P}$ and $A_{\rm T}$ represent the mass numbers of the projectile and target, respectively.

Taking the real potential $V(r)$ as an example, the perturbation of the potential $V_{\rm notch}$ can be expressed as

$$V_{\rm notch} = dV_0 f_{\rm V}(R',a,R) f_{\rm notch}(r,a',R'), \quad (3)$$

where R' and a' represent the position and width of the notch, d is the fraction by which the potential is reduced, and $f_{\rm notch}(r,a',R')$ is the derivative Woods-Saxon surface form factor:

$$f_{\rm notch}(r,a',R') = 4\exp\left(\frac{r-R'}{a'}\right) \Big/ \left[1+\exp\left(\frac{r-R'}{a'}\right)\right]^2. \quad (4)$$

Thus the perturbed real potential $V(r)_{\rm pert.}$ is:

$$V(r)_{\rm pert.} = V_0 f_{\rm V}(r,a,R) - V_{\rm notch}. \quad (5)$$

The perturbation for the imaginary potential can be derived with the same procedure. The typical perturbed potential with $r_0 = 1.25$ fm, $a = 0.65$ fm, $R' = 10$ fm, $a' = 0.1$ fm, and $d = 1.0$ is shown in Fig. 1.

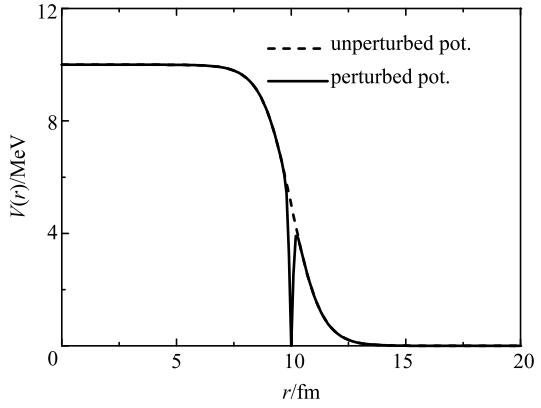

Fig. 1. The typical unperturbed potential (dashed curve) and perturbed potential (solid curve) with $r_0 = 1.25$ fm, $a = 0.65$ fm, $R' = 10$ fm, $a' = 0.1$ fm, and $d = 1.0$.

When the perturbation is located in the sensitive region, where the predicted cross section depends strongly on the details of the potential, the calculated elastic scattering angular distribution will change greatly. This means, when compared with the experimental data, there will be a dramatic variation in the χ^2 value. Conversely, at positions where the evaluated cross section is not sensitive to the potential, the perturbation has little influence on the calculated angular distribution. By means of the notch technique, the sensitive region of the nuclear potential can be presented visually and explicitly.

3 Sensitivity test of the notch technique

There may be several factors, from either the model parameters or the quality of the experimental data, which will affect the OMP sensitivity derived from the notch technique. The influences from some possible factors will be investigated in this section, to provide guidance for the application of the notch technique and the experimental procedure. The code FRESCO [13] was used to perform the optical model calculations.

3.1 Data generation

The elastic scattering data set of ^{16}O+^{208}Pb at $E_{\rm lab}(^{16}{\rm O}) = 129.5$ MeV [14], as shown in Fig. 2, was chosen to perform the sensitivity test. That is because this data is quite precise and measured in an extensive angle region but with small angle interval, and the ratio $d\sigma_{\rm el}/d\sigma_{\rm Ru}$ was measured down to 10^{-4} level. Meanwhile there is a clear picture for the interaction of this classic tightly-bound system, and the elastic scattering angular distribution can be described satisfactorily by the optical model. Moreover, at energy well above the Coulomb barrier, the nuclear force has a more significant effect, which is in favor of the investigation of the radial sensitivity of nuclear potential.

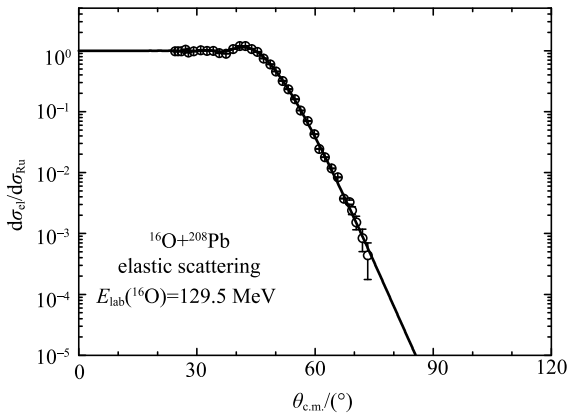

Fig. 2. Angular distributions of ^{16}O+^{208}Pb elastic scattering at $E_{\rm lab}(^{16}{\rm O}) = 129.5$ MeV [14]. The solid curve shows the fitting result with $V = 31.46$ MeV, $W = 30.0$ MeV, $r_{0i} = 1.25$ fm and $a_i = 0.65$ fm, where $i = V$ and W.

In order to completely eliminate the uncertainties from the experimental data, such as the statistics, angle step and range to be measured, a theoretical angular distribution was generated by fitting the experimental data with $r_{0i} = 1.25$ fm and $a_i = 0.65$ fm, as the solid curve shown in Fig. 2. This theoretical data can be regarded as an ideal data set with fixed angle step of 0.1° and statistical error of 1%. Considering the comparability with the actual experimental situation, the theoretical data is cut off at $\theta_{\rm c.m.} = 80°$, where $\mathrm{d}\sigma_{\rm el}/\mathrm{d}\sigma_{\rm Ru}$ is down to the 10^{-5} level. The following calculations and discussions are based on this equivalent angular distribution.

3.2 Dependence on model parameters

The dependence on model parameters was investigated first, including the perturbation parameters d and a', as well as the OMP parameters r_{0i} and a_i.

3.2.1 Perturbation parameters

The influence of the notch depth was investigated with the value of the reduced fraction d varied by a certain step size, with the notch width a' fixed at 0.05 fm. The variations of relative χ^2 at different d values are shown in Fig. 3. It can be seen that the greater the perturbations are, the larger the relative χ^2 values which will be brought in. Distinct peaks are observed for both the real and imaginary parts, corresponding to the radial sensitivity regions of the nuclear potential. For the real part, a main peak lies at the position around 11.92 fm, followed by a tiny peak in the inner region around 11.0 fm. For the imaginary part, two obvious peaks are observed: a major peak at around 12.20 fm and a minor peak at around 11.20 fm. There is little change in the sensitive region induced by the variation of d, except for the the lowest d value 0.2. In that case, a broad peak was presented at about 11.5 fm in the imaginary part, as shown in Fig. 3(b), which is incompatible with the others. It indicates that a too small reduced fraction of the perturbation may cause some spurious sensitivity region of the potential. A d value larger than 0.5 is recommended and d is fixed at 1.0 in the following discussions.

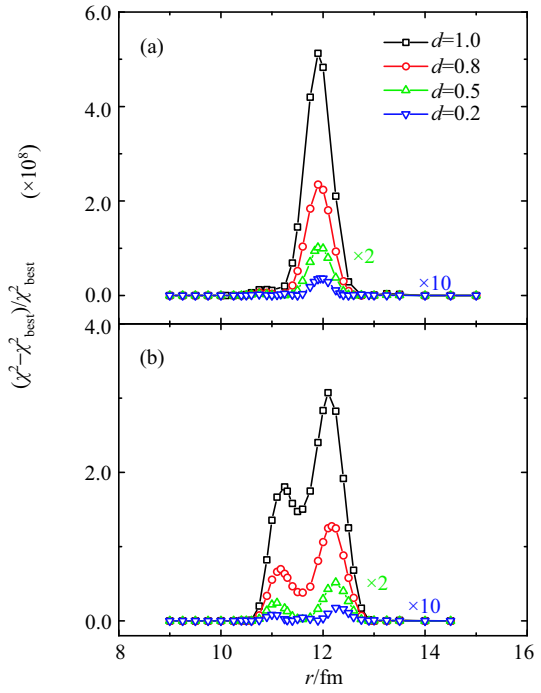

Fig. 3. (color online) The sensitivity functions for the real (a) and imaginary (b) parts of the potential with different d values. The "×2" and "×10" mean the corresponding results with the same color are multiplied by 2 and 10, for the convenience of comparison. The curves are used to guide the eye.

The notch width a' was set at 0.2, 0.1, 0.05 and 0.01 fm, respectively, and the corresponding sensitivity functions are shown in Fig. 4. It can be seen that a wider perturbation introduces a stronger influence, leading to a larger relative χ^2 value. However, the original distinct double-peaked structure in the imaginary part disappears when a large value of a' is adopted, replaced by one broad peak containing the gross information of the radial sensitivity. On the other hand, when $a' = 0.01$ fm, which is equal to the integration step size dr, three peaks emerge in the sensitivity function of the imaginary

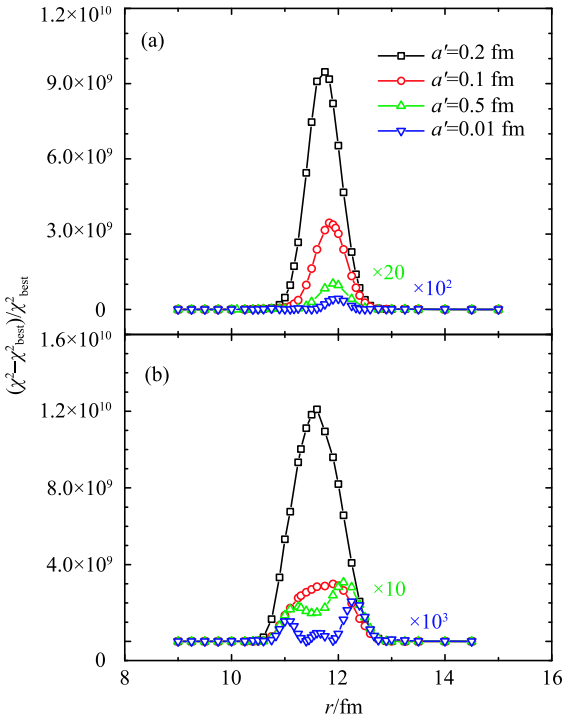

Fig. 4. (color online) The sensitivity functions for the real (a) and imaginary (b) parts of the potential with different perturbation width a' values. The curves are used to guide the eye.

part potential. As mentioned in Ref. [5], problems arise when a' becomes comparable to dr. Based on the above discussions, we argue that a smaller a' is beneficial to extract the fine information on the sensitivity of the radial potential, but it should not be too close to the integration step size. The a' value of 0.05 fm, about 5 times the integration step dr, is used in the following results.

3.2.2 OMP parameters

With the fixed perturbation parameters, further investigations were performed on the OMP parameters. First, the ideal angular distribution was fitted with r_{0i} fixed at 1.20, 1.25 and 1.30 fm, respectively, and the results are shown in Fig. 5. Second, the fitting procedure was repeated but with a_i fixed at 0.60, 0.65 and 0.70 fm, respectively, and the results are shown in Fig. 6. One can see that relative χ^2 values between the main (major) peaks and tiny (minor) peaks for the real (imaginary) part vary obviously with r_{0i} and a_i. However, nearly the same sensitive regions were determined by those OMP parameter sets, although the relative sensitivity differed from each other. Therefore, it can be concluded that the sensitive region determined by the notch technique is nearly model-independent.

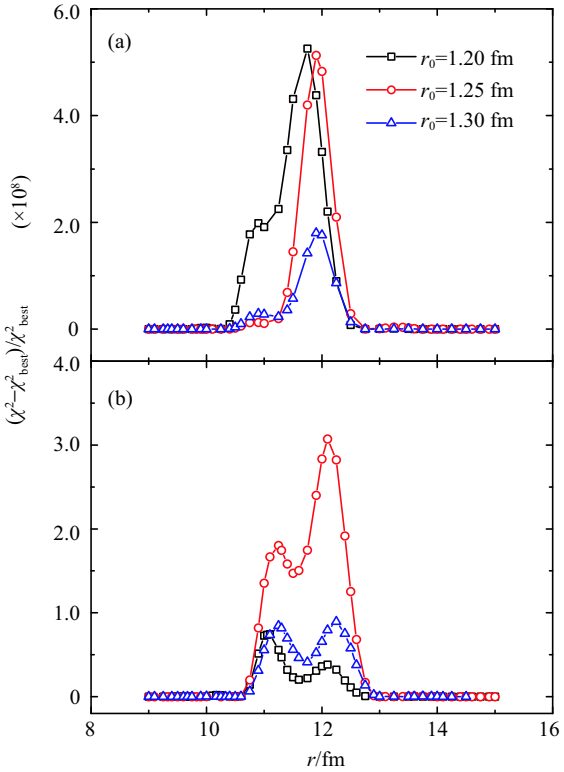

Fig. 5. (color online) The sensitivity functions for the real (a) and imaginary (b) parts of the potential with different OMP parameters derived with fixed r_{0i}. The curves are used to guide the eye.

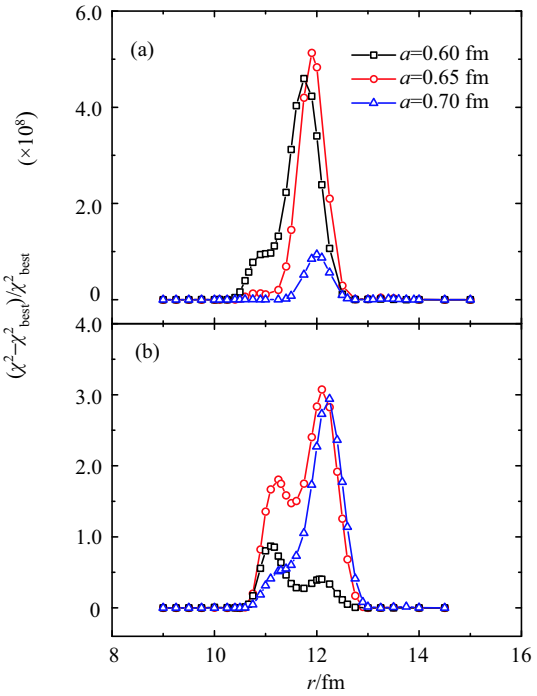

Fig. 6. (color online) The sensitivity functions for the real (a) and imaginary (b) parts of the potential with different OMP parameters derived with fixed a_i. The curves are used to guide the eye.

3.3 Dependence on experimental data

After the investigation of model dependence, a further sensitivity test on the experimental data was performed, to assess the influence arising from the quality of the data-set, and provide some guidance on the experimental measurements.

3.3.1 Angle interval

A fine angle interval may be useful in determining a reliable OMP parameter set but it is time consuming, especially for RIB experiments. In order to check its influence on the sensitive region, different angle intervals $\theta_{\rm int.}$, i.e. $\theta_{\rm int.}=0.1^\circ, 1^\circ, 5^\circ$ and 10° were adopted for the ideal data set. The corresponding sensitivity functions are shown in Fig. 7. It can be seen that bigger $\theta_{\rm int.}$ introduces a larger χ^2 value. There are no obvious changes in the structures of the sensitivity functions for both the real and imaginary parts. It demonstrates that on the premise of large angle-region as well as good statistics, the sensitive region can be determined accurately even by a few experimental data points. This conclusion is important for the elastic scattering measurements with RIBs, whose angular distributions usually have only a few points due to the limits of the intensity and quality of the available RIBs [15, 16]. However, it should be kept in mind that this indication is only available for heavy target systems, whose angular distribution of

elastic scattering is almost structureless. With light nuclear systems, whose elastic scattering angular distribution presents strong interference patterns, a fine measurement is necessary to describe the detailed structure of the angular distribution.

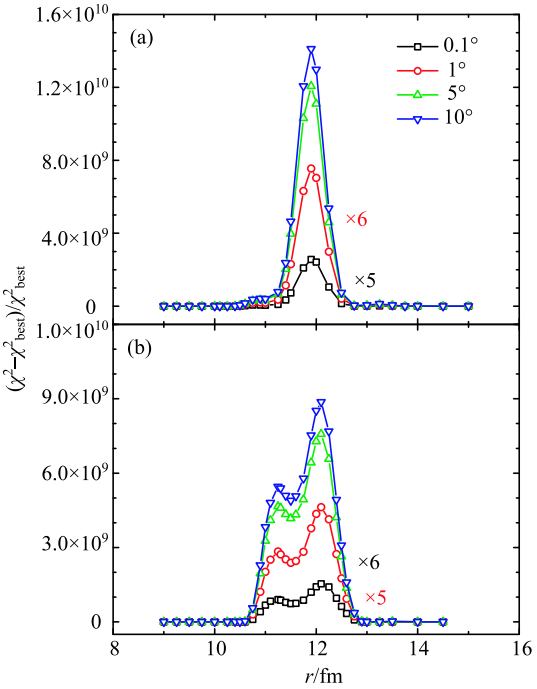

Fig. 7. (color online) The sensitivity functions for the real (a) and imaginary (b) parts of the potential for experimental data set with different $\theta_{int.}$. The curves are used to guide the eye.

3.3.2 Angle region

In principle, the wider angular region measured, the tighter the constraint that can be achieved on the OMP parameters. However, it is hard to extend the experimental data to large angles where the cross section become very low for elastic scattering, especially at high energies. From the physics point of view, data at the back angles may provide more information on the inner potential. In order to inspect the influence of angular region measured, the ideal data were divided into five sets: the first set contains the data down to $d\sigma_{el}/d\sigma_{Ru} = 0.25$ at the grazing angle, corresponding to one-half of the transmission coefficient; the second set contains the data down to $d\sigma_{el}/d\sigma_{Ru} = 0.025$, etc., until the fifth set, which contains all the data points cut off at $\theta_{c.m.} = 80°$, where $d\sigma_{el}/d\sigma_{Ru} = 6.0\times10^{-5}$. Results of the sensitivity test for each data set are shown in Fig. 8. Distinct peaked structures are observed for both the real and imaginary potential parts. In order to evaluate quantitatively the influences of the data region measured, the main peak of the real part and major peak of the imaginary part were fitted by a Gaussian function, respectively. Values of the center position as well as its sigma width are listed in Table 1.

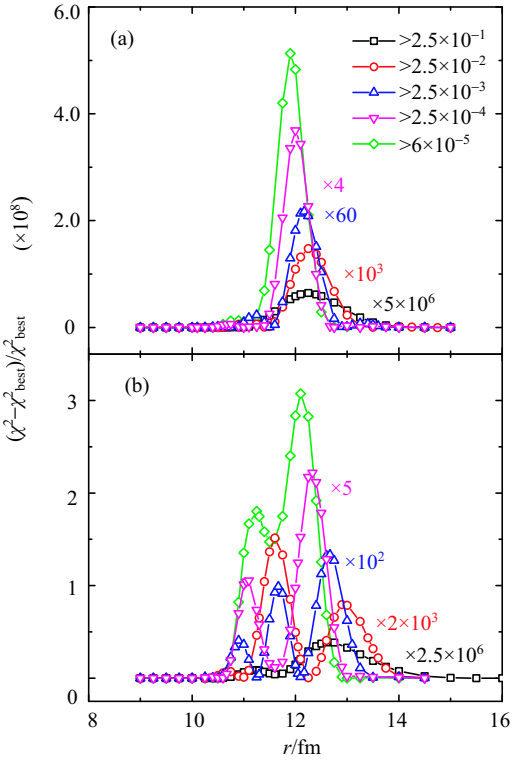

Fig. 8. (color online) The sensitivity functions for the real (a) and imaginary (b) parts of the potential for experimental data set with different $d\sigma_{el}/d\sigma_{Ru}$ extensions. The curves are used to guide the eye.

Table 1. The center(sigma) values of the peaks observed in Fig. 8. The real and imaginary correspond to the main peak of the real part and the major peak of the imaginary part, respectively. The value of the center is in the unit of fm.

data range	real	imaginary
$>2.5\times10^{-1}$	12.31(0.56)	12.76(0.57)
$>2.5\times10^{-2}$	12.29(0.34)	13.02(0.34)
$>2.5\times10^{-3}$	12.17(0.25)	12.68(0.25)
$>2.5\times10^{-4}$	12.01(0.23)	12.33(0.25)
$>6.0\times10^{-5}$	11.91(0.25)	12.10(0.31)

For the first data set, containing only the data with $d\sigma_{el}/d\sigma_{Ru} > 0.25$, the nuclear force just begins to take effect, thus it is difficult to obtain accurate information on the nuclear potential, so a very broad peak presents. As we extend the data to larger angles, the effects of the nuclear force begin to increase, and more detailed information can be extracted. Meanwhile both the main peak of the real part and the major peak of the imaginary part systematically move inward as the angle goes backward. However, considering the peripheral nature of

elastic scattering, the inner potential cannot be probed when the distance is shorter than a certain value.

Moreover, the lower the cross section of elastic scattering measured, the larger the relative χ^2 value that will be obtained. The relative χ^2 value of the fifth set is 10^7 times larger than that of the first set. As mentioned above, the value of relative χ^2 represents the sensitivity degree of the OMP parameters to the elastic scattering data. Such a large relative χ^2 value demonstrates that an adequate constraint can be achieved for the OMP parameters within the sensitive region when the measurement reaches a very low cross section.

3.4 Discussion

The ideal test provides a solid foundation for the application of the notch technique. With appropriate parameters for the notch and OMP, the physical meanings of sensitivity peaks can be understood. In order to demonstrate this clearly, several available radii and distances, e.g. the radius of the interaction potential $R_{\rm int}$, Coulomb barrier radius $R_{\rm B}$, strong absorption radius $R_{\rm sa}$, as well as the distance D_0 where the nuclear force begins to take effect, are labeled in Fig. 9 by vertical lines. $R_{\rm sa}$ is the radius where the observed cross section has fallen to one-fourth of the Rutherford value; and D_0 corresponds to the distance of $\mathrm{d}\sigma_{\rm el}/\mathrm{d}\sigma_{\rm Ru}=0.98$. One can find that even for data down to $\mathrm{d}\sigma_{\rm el}/\mathrm{d}\sigma_{\rm Ru}=6.0\times10^{-5}$, the main sensitivity regions are located around 12.0 fm, far larger than $R_{\rm int}$, 10.56 fm, demonstrating that the OMPs determined by the elastic scattering are only sensitive to surface regions. And as mentioned in Ref. [6], because of the strong absorption, it seems unlikely that much light can be shed on the behavior of the real potential in the deep interior region with measurements of heavy-target system elastic scattering.

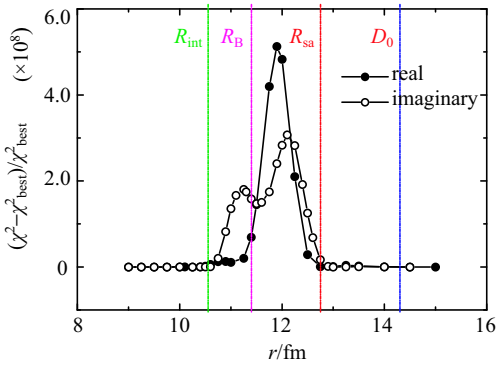

Fig. 9. (color online) The sensitivity functions of the real (full circle) and imaginary (hollow circle) parts with the data range down to $\mathrm{d}\sigma_{\rm el}/\mathrm{d}\sigma_{\rm Ru}=6.0\times10^{-5}$. The interaction radius $R_{\rm int}$, Coulomb barrier radius $R_{\rm B}$, strong absorption radius $R_{\rm sa}$, and the distance D_0 are shown by vertical lines. See the text for details.

For the imaginary part, two distinct peaks are observed. The major one lies around $R_{\rm sa}$, corresponding to the surface absorption process; the minor peak locates around $R_{\rm B}$, which should be responsible for the volume absorption, i.e. the capture reaction process. For the real part, the main peak is located near $R_{\rm sa}$, followed by a tiny inner peak, which lies inside $R_{\rm B}$. Both of the two real-part peaks are located inside the corresponding imaginary ones. The main peak of the real part arises from the direct scattering process. The origin of the tiny peak was thought to be associated with the far-side interference effect [5, 8]. In order to check the reliability of this explanation, decomposition of the far- and near-side scattering was performed with the method developed in Ref. [17], and the result is shown in Fig. 10. One can find that the far-side scattering is almost negligible for the whole angular range, indicating that the tiny peak does not originate from interference between the far- and near-side components. Considering that the location of the tiny peak is inside $R_{\rm B}$, we believe this peak should be the result of resonance scattering, where the compound nucleus has been formed.

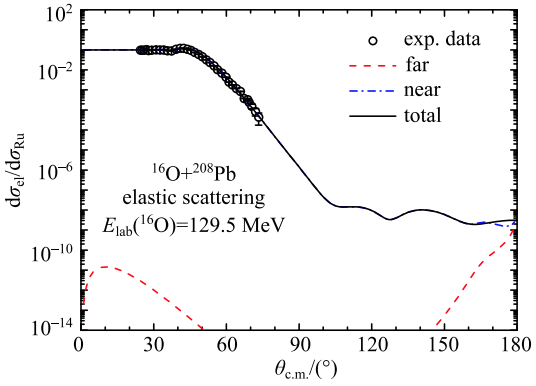

Fig. 10. (color online) The elastic angular distribution of ^{16}O+^{208}Pb at $E_{\rm lab}(^{16}{\rm O})$=129.5 MeV. Open circles represent the experimental data. The best-fit result is shown by the solid curve. Decomposition of the far- and near-side are shown by the dashed and dot-dashed curves, respectively.

4 Summary and conclusions

The sensitivity of the notch technique to the parameters of the perturbation and OMP, as well as the experimental data, were investigated in the present work. Through the ideal test we can draw conclusions as below: 1) a sufficiently large reduced fraction d can help to obtain accurate information on the sensitive region, and d=1.0 is the adopted value; 2) the width of the perturbation a' should be several times the integration step dr, as an inappropriate large or small value of a' will lead to a spurious result; 3) the notch technique is almost independent of the OMP parameters; 4) for heavy-target

nuclear systems, on the premise of large angle-region as well as good statistics measurement, there is no need for a great many experimental data points to ensure the reliability of the sensitive region extracted. This may aid in optimizing the setup of elastic scattering measurements, especially for the experiments with RIBs; 5) the relative inner information of the nuclear potential can be derived when the measurement is extended to a lower elastic scattering cross section. However, the deep interior region of the nuclear potential is still invisible through the elastic scattering measurement due to the effect of strong absorption.

With these detailed investigations of the notch technique, we can further apply this method to research on the radial sensitivities of both tightly- and weakly-bound nuclear systems, which are essential issues in the studies of the OMP.

References

1 M. E. Brandan, G. R. Satchler, Phys. Rep, **285**: 143 (1997)
2 N. Keeley, N. Alamanos, K. W. Kemper, K. Rusek, Prog. Part. Nucl. Phys., **63**: 396 (2009)
3 N. Keeley, R. Raabe, N. Alamanos, J. L. Sida, Prog. Part. Nucl. Phys., **59**: 579 (2007)
4 G. Igo, Phys. Rev. Lett., **1**: 72 (1958)
5 J. G. Cramer, R. M. DeVries, Phys. Rev. C, **22**: 91 (1980).
6 P. J. Moffa, C. B. Dover, J. P. Vary, Phys. Rev. C, **13**: 147 (1976)
7 C. J. Lin, J. C. Xu, H. Q. Zhang et al, Phys. Rev. C, **63**: 064606 (2001)
8 D. Roubos, A. Pakou, N. Alamanos, K. Rusek, Phys. Rev. C, **73**: 051603(R) (2006)
9 M. H. Macfarlane, S. C. Pieper, Phys. Lett. B, **103**: 169 (1981)
10 M. Biswas, Phys. Rev. C, **77**: 017602 (2008)
11 F. Michel, J. Albinski, P. Belery et al, Phys. Rev. C, **28**: 1904 (1983)
12 J. D. Brown, E. Lau, S. Roman, J. Phys. G: Nucl. Phys. **10**: 1391 (1984)
13 I. J. Thompson, Comp. Phys. Rep., **7**: 167 (1988)
14 J. B. Ball, C. B. Fulmer, E. E. Gross et al, Nucl. Phys. A, **252**: 208 (1975)
15 E. F. Aguilera, J. J. Kolata, F. D.Becchetti et al, Phys. Rev. C **63**: 061603(R) (2001)
16 E. F. Aguilera, E. Martinez-Quiroz, D. Lizcano et al, Phys. Rev. C, **79**: 021601(R) (2009)
17 R. Anni, J. N. L. Connor, C. Noli, Phys. Rev. C, **66**: 044610 (2002)